LAP2α-binding protein LINT-25 is a novel chromatin-associated protein involved in cell cycle exit

Nana Naetar[1], Sabine Hutter[1], Daniela Dorner[1], Thomas Dechat[1], Barbara Korbei[1], Josef Gotzmann[1], Hartmut Beug[2] and Roland Foisner[1,*]

[1]Max F. Perutz Laboratories, Department of Medical Biochemistry, Medical University of Vienna, Dr. Bohr-Gasse 9 and [2]Institute of Molecular Pathology, Vienna Biocenter, Dr. Bohr-Gasse 7, A-1030 Vienna, Austria

*Author for correspondence (e-mail: roland.foisner@meduniwien.ac.at)

Accepted 4 January 2007
Journal of Cell Science 120, 737-747 Published by The Company of Biologists 2007
doi:10.1242/jcs.03390

Summary

Lamina-associated polypeptide 2α (LAP2α) is a nuclear protein dynamically associating with chromatin during the cell cycle. In addition, LAP2α interacts with A-type lamins and retinoblastoma protein and regulates cell cycle progression via the E2F-Rb pathway. Using yeast two-hybrid analysis and three independent in vitro binding assays we identified a new LAP2α interaction partner of hitherto unknown functions, which we termed LINT-25. LINT-25 protein levels were upregulated during G1 phase in proliferating cells and upon cell cycle exit in quiescence, senescence and differentiation. Upon cell cycle exit LINT-25 accumulated in heterochromatin foci, and LAP2α protein levels were downregulated by proteasomal degradation. Although LAP2α was not required for the upregulation and reorganization of LINT-25 during cell cycle exit, transient expression of LINT-25 in proliferating cells caused loss of LAP2α and subsequent cell death. Our data show a role of LINT-25 and LAP2α during cell cycle exit, in which LINT-25 acts upstream of LAP2α.

Supplementary material available online at
http://jcs.biologists.org/cgi/content/full/120/5/737/DC1

Key words: Cell cycle, Chromatin, Differentiation, Lamins, Quiescence, Senescence

Introduction

Lamins are nuclear-specific intermediate filament proteins that form a filamentous scaffold structure underneath the inner nuclear membrane called the lamina, in multicellular eukaryotes (Goldman et al., 2002; Gruenbaum et al., 2005; Stuurman et al., 1998). Whereas B-type lamins are essential for cell viability, A-type lamins are predominantly expressed in terminally differentiated cells (Cohen et al., 2001). A small pool of A-type lamins is also found in the nucleoplasm (Bridger et al., 1993; Dechat et al., 2004; Hozak et al., 1995; Moir et al., 2000b), where it may function in chromatin organization and gene expression (Mattout-Drubezki and Gruenbaum, 2003), DNA replication (Moir et al., 2000a), RNA Pol II-dependent transcription (Spann et al., 2002), and cell cycle progression and differentiation (Ivorra et al., 2006; Johnson et al., 2004; Markiewicz et al., 2005; Van Berlo et al., 2005).

Lamina-associated polypeptide (LAP)2α interacts with the nucleoplasmic pool of A-type lamins (Dechat et al., 2000a). It is one of six alternatively spliced isoforms of the *LAP2* gene (Dechat et al., 2000b) and is structurally and functionally unique among the LAP2 family members. LAP2α shares only the N-terminus with the other LAP2 proteins and contains a unique C-terminus. Furthermore, LAP2α is localized exclusively in the nucleoplasm (Dechat et al., 1998; Vlcek et al., 1999), whereas other isoforms, such as LAP2β, γ, δ and ϵ are inner nuclear membrane proteins (Berger et al., 1996; Harris et al., 1994) that bind lamin B (Foisner and Gerace, 1993; Furukawa and Kondo, 1998). Nucleoplasmic complexes of LAP2α and lamin A/C interact with a tumor suppressor, the retinoblastoma (Rb) protein (Markiewicz et al., 2002; Ozaki et al., 1994) and regulate the expression of E2F-Rb-dependent target genes during cell cycle exit and differentiation by unknown mechanisms (Dorner et al., 2006).

Intriguingly, mutations in the lamin A gene cause a heterogeneous group of inherited human diseases, collectively called laminopathies, which affect heart, skeletal muscle, adipose, skin and nerve cells (Burke and Stewart, 2002; Gruenbaum et al., 2005; Hutchison and Worman, 2004) or lead to premature ageing (Mounkes and Stewart, 2004). Also, mutations in LAP2α have been linked to cardiomyopathy (Taylor et al., 2005). The molecular basis of these diseases may involve structural defects in the disease-linked mutated protein variants, but in view of the potential role of LAP2α and lamin A in cell cycle control, mutations in these proteins could also affect the proliferation and differentiation of adult stem cells, leading to impaired tissue regeneration (Gotzmann and Foisner, 2006; Hutchison and Worman, 2004).

LAP2α has also been implicated in higher order chromatin organization during both the cell cycle and differentiation. It interacts with DNA and chromatin through several domains. Like all LAP2 proteins, LAP2α contains an N-terminal ~40-residue long structural motif (termed the LEM domain), which is also found in the inner nuclear membrane proteins MAN1, emerin (Lin et al., 2000) and LEM2 (Brachner et al., 2005). The LEM domain interacts with the highly conserved DNA-binding protein barrier-to-autointegration factor (BAF) (Segura-Totten et al., 2002). In addition, all LAP2 proteins

contain a LEM-like motif at the very N-terminus that binds DNA (Cai et al., 2001). The unique C-terminus of LAP2α was shown to mediate the association of LAP2α with telomeres during early stages of post-mitotic nuclear assembly (Dechat et al., 2004; Vlcek et al., 1999).

To gain further insight into the molecular mechanisms of LAP2α functions in chromatin organization and cell cycle control, we aimed at identifying novel LAP2α interaction partners in a yeast two-hybrid screen. Here we report a novel 25 kDa protein termed LAP2α interactor-25 (LINT-25) that binds to the LAP2α-specific C-terminus. Intriguingly, LINT-25 is upregulated and relocalized to heterochromatin foci upon reversible and irreversible cell cycle exit, concomitant with a downregulation of LAP2α. Our studies suggest that the interaction of LINT-25 and LAP2α may function at the transition from the active cell cycle to the non-cycling state.

Results

LINT-25 is a novel interaction partner of LAP2α

In a yeast two-hybrid screen, using a HeLa cDNA library and the unique LAP2α-specific C-terminus as a bait, we identified Opa-interacting protein 5 (OIP5) as a potential binding partner of LAP2α. OIP5 was previously found by yeast two-hybrid analysis to interact with *Neisseria gonorrhoeae* opacity-associated (Opa) proteins (Williams et al., 1998). Opa proteins are found in the outer membrane of *N. gonorrhoeae* and are involved in gonococcal adhesion to and invasion of human epithelial cells. Neither the role of OIP5 in the Opa-mediated infection nor its physiological functions in non-infected cells were known. Our two-hybrid clone matched nucleotides 67-990 of OIP5 [TIGR (the Institute for Genomic Research) accession no. THC2238209], including the complete coding region except for the first two N-terminal amino acids (Fig. 1A). In view of the lack of biochemical and cell biological data on the Opa-OIP5 interaction, as opposed to the detailed interaction analysis between OIP5 and LAP2α shown here, we renamed the protein LINT-25 (for LAP2α-interactor of 25 kDa) and use this term throughout the manuscript.

The human *LINT-25* gene localizes to chromosome region 15q15.1 (NCBI GeneID 11339) including 5 exons and spanning approximately 23 kb. The longest full-length LINT-25 cDNA in the database (1214 bp, TIGR THC2238209) has been assembled from ESTs from diverse tissues including testis and lymph nodes. An open reading frame was predicted between nucleotides 61 and 750, encoding a protein of 229 amino acids with a calculated molecular mass of 24.7 kDa. A BLAST homology search in the gene indices databases of TIGR revealed homologous protein sequences in *Mus musculus* and *Rattus norvegicus* with more than 70% identity and approximately 80% similarity to human LINT-25 (Fig. 1A). Furthermore, translated ESTs from *Gallus gallus*, *Xenopus laevis* and *Danio rerio* showed 34-45% identity and 55-61% similarity with human LINT-25 in the central domain. N- and C-termini of the LINT-25 orthologues were less conserved and of different sizes (Fig. 1A). In addition, we found a human cDNA encoding a protein of unknown function, named C21orf45 for chromosome 21 open reading frame 45 (TIGR accession no THC2246127), parts of which were 24% identical and 43% similar to the LINT-25 C-terminus (Fig. 1A). Database sequence analysis of human LINT-25 predicted a coiled-coil domain at the C-terminal end of the central conserved region (residues 192-219; Fig. 1A). Apart from this we did not detect any other predicted functional or structural domains.

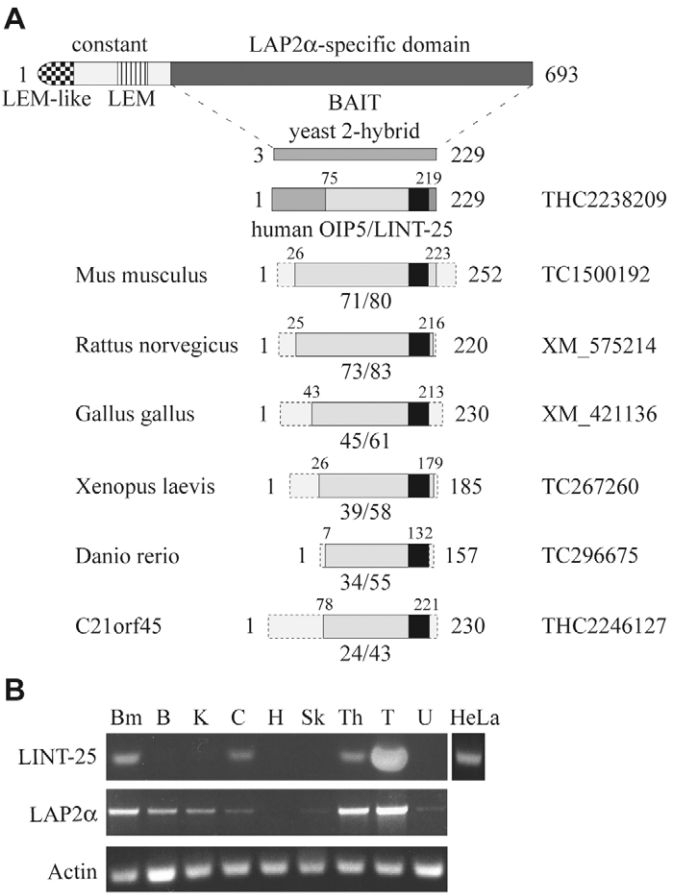

Fig. 1. LINT-25 is a novel interaction partner of LAP2α. (A) Diagram of the domain organization of LAP2α, full-length human OIP5/LINT-25 (229 residues, TIGR THC2238209) and the yeast two-hybrid fragment identified using LAP2α-specific C-terminus as bait. The light gray box in human LINT-25 (residues 75-219) delineates conserved regions found also in protein sequences in *Mus musculus* (TIGR TC1500192), *Rattus norvegicus* (GB XM_575214), *Gallus gallus* (GB XM_421136), *Xenopus laevis* (TIGR TC267260), *Danio rerio* (TIGR TC296675) and *Homo sapiens* (TIGR THC2246127) with dotted lines showing the predicted full-length proteins. The black rectangle represents a predicted coiled-coil domain. Accession numbers given are from the Institute for Genomic Research (TIGR) and from GenBank (GB). The two numbers below each bar indicate the percentage identity and similarity, respectively, to human LINT-25 protein sequence. (B) RT-PCR analyses of LINT-25, LAP2α, and actin mRNA as control, using mRNAs from the indicated human tissues or cell line: bone marrow (Bm), brain (B), colon (C), heart (H), kidney (K), skeletal muscle (Sk), thymus (Th), testis (T) and uterus (U). An ethidium bromide-stained gel of PCR fragments is shown.

To study the relative expression levels of LINT-25 and LAP2α, we performed semiquantitative reverse transcription (RT)-PCR using mRNAs from nine human tissues (Fig. 1B). LINT-25 mRNA levels were highest in testis, followed by bone marrow, thymus and colon, whereas brain, kidney, heart, skeletal muscle and uterus, showed no signal. Control reactions

with actin-specific primers confirmed the presence of equal amounts of mRNA in these samples. Strikingly, the LAP2α expression pattern was similar to that of LINT-25, revealing strongest expression in bone marrow, thymus and testis, and no detectable expression in skeletal muscle and heart. Thus, LINT-25 and LAP2α could well be involved in the formation of common complexes in these tissues, most of which intriguingly are tissues with a high regenerative and/or proliferative capacity.

LINT-25 and LAP2α interact directly in vitro

To confirm direct binding of LINT-25 to LAP2α, we performed three independent in vitro binding assays, co-immunoprecipitations using either recombinant or in vitro translated, ^{35}S-labeled proteins and blot overlays. In the first co-immunoprecipitation assay, recombinant His-tagged full-length LINT-25 and LAP2α were incubated alone or together, and LAP2α complexes were pulled down with LAP2α antibody. Western blot analysis revealed LINT-25 in the immunoprecipitates in the presence, but not in the absence of LAP2α (Fig. 2A). We also performed a second co-immunoprecipitation assay using [^{35}S]methionine-labeled in vitro translated proteins (Fig. 2B). Unlike the control (DMEM), LAP2α antibodies co-precipitated LAP2α and a significant fraction of LINT-25, whereas LINT-25 alone was not precipitated above background levels by the antibody. The relative amount of LAP2α-bound LINT-25 was lower than the one obtained using recombinant proteins, but was significant and clearly above background levels. ^{35}S-labeled LINT-25 did not co-precipitate with labeled LAP2β nucleoplasmic domain under the same conditions, confirming specificity of the LINT-25-LAP2α interaction (Fig. 2B, right).

For blot overlays, His-tagged, recombinant LINT-25 was transblotted onto nitrocellulose and detected with the protein stain Ponceau S or a His-tag-specific probe (Fig. 2C, left panels), or overlaid with recombinant LAP2α or buffer as control. Immunoblot analysis of the overlaid samples with LAP2α antibody revealed LAP2α binding to LINT-25 (Fig. 2C, right panels). Blot-immobilized His-tagged LAP2β as a negative control did not interact with overlaid LAP2α (data not shown). Thus, three independent in vitro binding assays revealed direct and specific binding of LAP2α to LINT-25.

Endogenous LINT-25 is a nuclear and chromosome-associated protein

In order to analyze LINT-25 in vivo we generated a polyclonal rabbit antiserum against recombinant LINT-25. The affinity-purified serum detected two bands of 25 kDa and 50 kDa in recombinant LINT-25 samples and in cell lysates of various human cell lines, probably representing monomeric and dimeric LINT-25 (see supplementary material Fig. S1A-C). Using reducing and/or alkylating agents during cell lysis we found that endogenous LINT-25 predominantly exists in a reduced form in cells (see supplementary material Fig. S1D), but is readily oxidized during lysis because of the high number of cysteines in the polypeptide sequence (9 of 229 residues). Despite the general use of reducing conditions during sample preparation throughout this study we detected variable amounts of monomeric versus dimeric LINT-25 after cell lysis in different experiments.

To investigate the cellular distribution and localization of

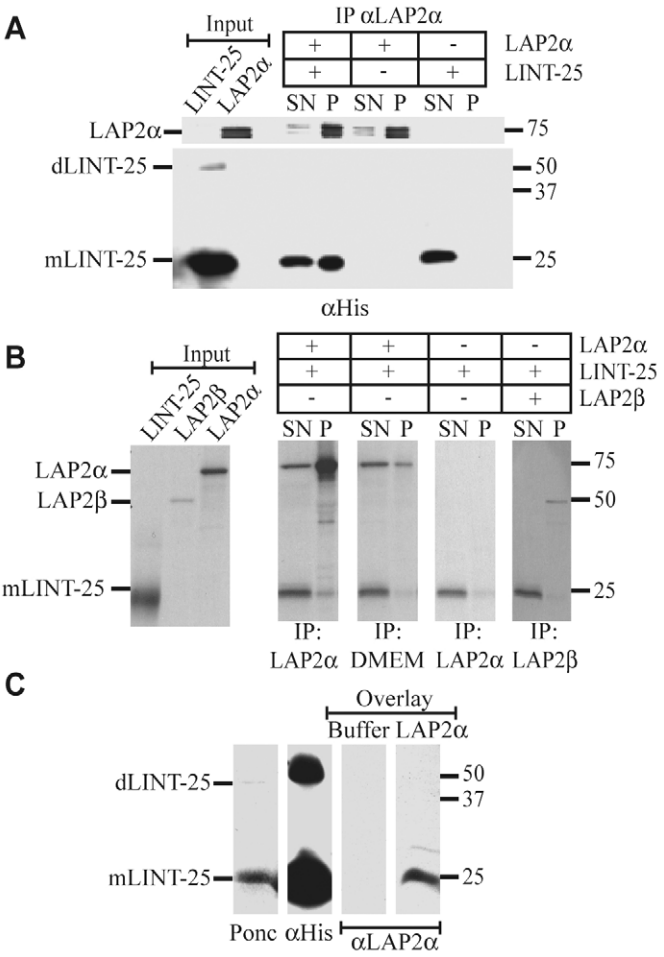

Fig. 2. LINT-25 and LAP2α interact in vitro. (A) His-tagged, recombinant LINT-25 and LAP2α were incubated alone or together and mixed with immobilized LAP2α antibody. Immunoprecipitates (P) and supernatants (SN) were analyzed by immunoblotting detecting LAP2α (upper panel) and the His-Tag (lower panel). Input represents 10% of protein used for IPs. (B) In vitro translated, [^{35}S]methionine-labeled LINT-25 was incubated alone or together with in vitro translated and labeled LAP2α or LAP2β1-408 and mixed with immobilized LAP2α- and LAP2β antibodies (IP) or hybridoma medium (DMEM) as a control. Immunoprecipitates (P) and supernatants (SN) were analyzed by SDS-PAGE and autoradiography. Input represents 2% of protein used for IP. Note, that the signals of the different protein bands do not reflect the relative protein levels due to different numbers of methionines in the proteins' primary sequences. (C) Recombinant LINT-25 was transblotted to nitrocellulose, stained with Ponceau S (Ponc), or detected with αHis-tag reagent (αHis) or overlaid with recombinant LAP2α or buffer. Bound LAP2α was detected using LAP2α antibodies (αLAP2α). Numbers indicate molecular masses of marker proteins in kDa; mLINT-25, monomeric LINT-25; dLINT-25, dimeric LINT-25.

LINT-25 we analyzed nuclear and cytoplasmic fractions by western blotting. LINT-25 was detected exclusively in the nuclear fraction, together with A-type lamins and LAP2 proteins (Fig. 3A). However, unlike the majority of A/C-type lamins, LAP2α and LAP2β, LINT-25 was completely soluble

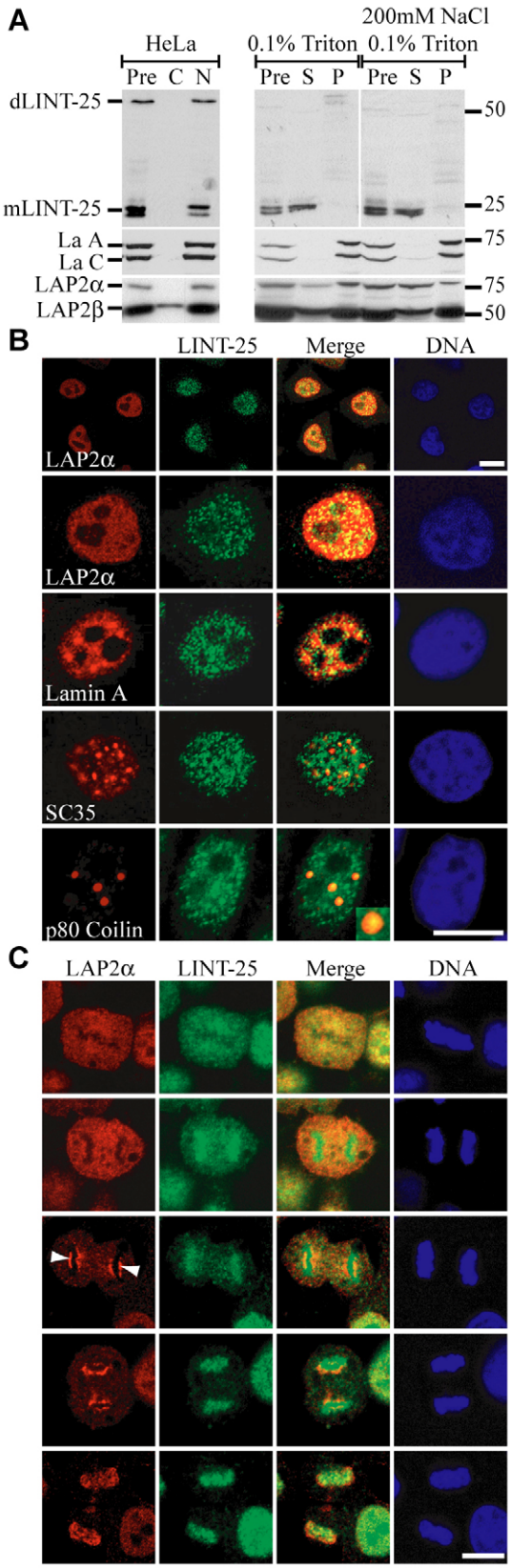

Fig. 3. LINT-25 localizes to the nucleus and associates with chromatin during mitosis. (A) HeLa cells were lysed in hypotonic buffer with iodoacetamide (IAA) (left panel), and total lysates (Pre), nuclear (N) and cytoplasmic (C) fractions were analyzed by immunoblotting using antibodies against LINT-25, lamin A/C and LAP2 (right panel). HeLa cells were lysed in culture dishes in buffer with the indicated concentrations of Triton X-100 and salt and total lysates (Pre), insoluble pellet fractions (P) and supernatants (S) were analyzed by immunoblotting. Note that the LINT-25 double band is caused by additional alkyl-groups resulting from the IAA treatment (see also supplement). Numbers indicate molecular masses of marker proteins in kDa; mLINT-25, monomeric LINT-25; dLINT-25, dimeric LINT-25; La, lamin. (B,C) HeLa cells were fixed with formaldehyde and double-stained for immunofluorescence microscopy using LINT-25 antiserum and antibodies against the indicated antigens. DNA was stained with Hoechst dye. Confocal images of interphase cells (B) or various stages of mitosis (C) are shown. Arrowheads indicate outer core regions. Bars, 10 μm.

in hypotonic buffer containing 0.1% Triton X-100 (Fig. 3A). Thus, LINT-25 is a nuclear protein, but is not part of a stable nucleoskeletal structure, like lamins and the majority of LAP2α, which were soluble only in high-salt Triton X-100 buffer. Immunofluorescence microscopy using affinity-purified LINT-25 antibody revealed LINT-25 in a mostly punctuate distribution throughout the nucleoplasm of interphase cells, partially overlapping with LAP2α (Fig. 3B). The LINT-25 structures did neither significantly overlap with SC-35-containing splicing complexes or speckles stained with a monoclonal lamin A/C antibody (Jagatheesan et al., 1999). Intriguingly, all the analyzed Cajal bodies identified by the presence of p80 coilin (Matera, 1999) contained LINT-25 (Fig. 3B, insert in bottom row), but the physiological significance of this observation remains unclear.

LAP2α has been shown to form defined structures on chromatin during early stages of post-mitotic nuclear reassembly (Dechat et al., 2004). Therefore, we wondered whether LINT-25 may also be recruited to these structures. LINT-25 was dispersed throughout the cytoplasm in metaphase and early anaphase (Fig. 3C) and associated with chromatin in late anaphase to early telophase. However, whereas LAP2α formed 'core structures' on chromatin adjacent to the spindle pole and the mid-spindle microtubules (Fig. 3C, arrowheads), LINT-25 localized uniformly throughout the entire chromatin. Thus, LINT-25 is a chromatin-binding protein associating with chromosomes early in assembly, but may not be involved in the formation of LAP2α-specific core regions (Dechat et al., 2004).

LINT-25 is upregulated and translocated to chromocenters in quiescence and senescence

Considering the recently reported function of LAP2α in controlling cell cycle progression and differentiation (Dorner et al., 2006), as well as the predominant expression of both LAP2α and LINT-25 in tissues with high poliferative potential, we wondered whether LINT-25 may be involved in LAP2α-mediated cell cycle-regulatory pathways. To address this possibility, we analyzed telomerase-immortalized fibroblasts (BJ1), which can be forced into quiescence by serum starvation. Cultivation in low serum medium for 7-9 days forced cells to exit a cycling state, as indicated by the loss of expression of proliferation markers (Ki67 and PCNA) (Fig. 4A,B). Both immunoblot analyses of cell lysates and the comparison of quiescent and proliferating cells by

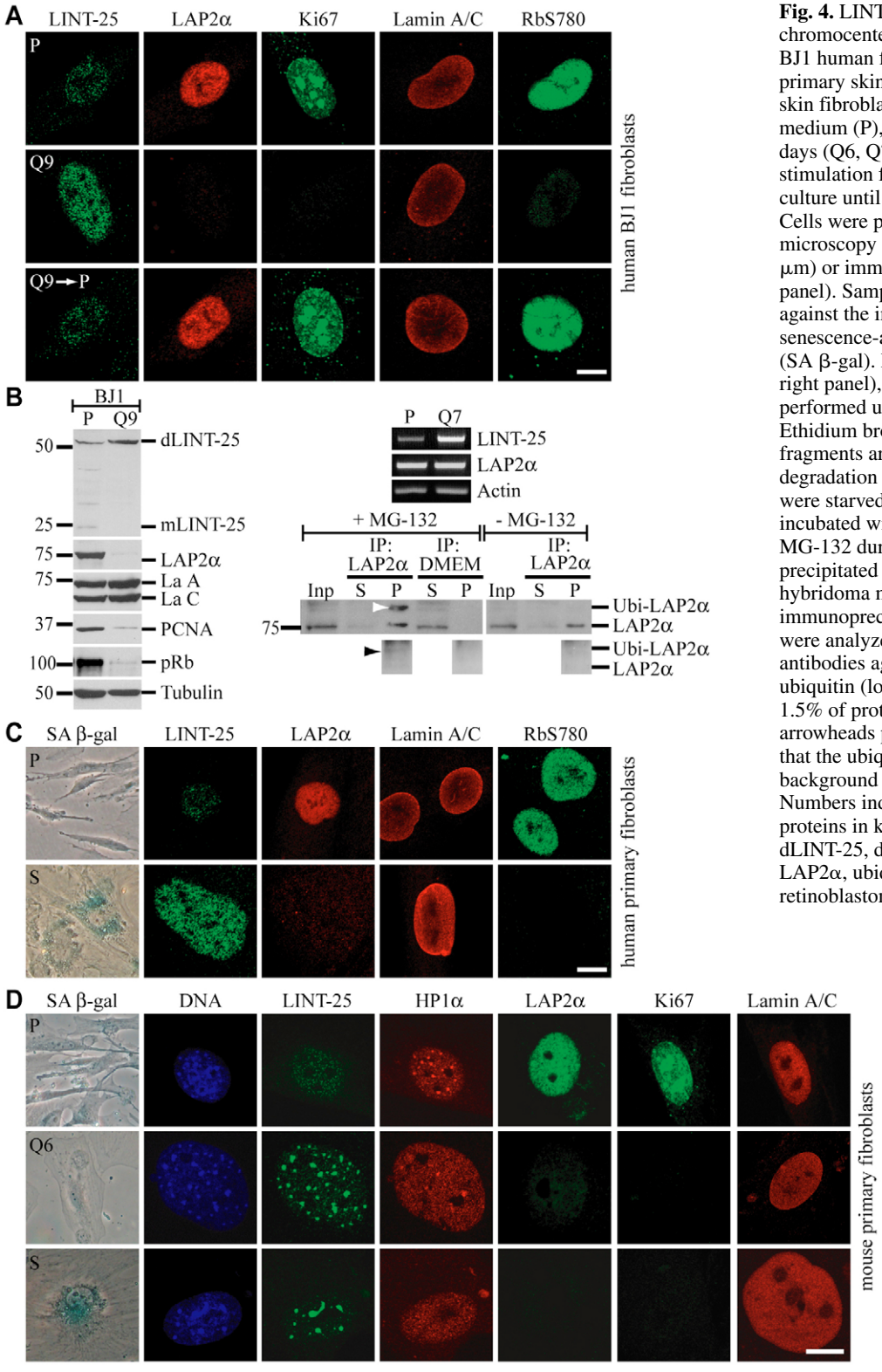

Fig. 4. LINT-25 is upregulated and translocated to chromocenters in non-proliferating fibroblasts. BJ1 human foreskin fibroblasts (A,B), human primary skin fibroblasts (C) and mouse primary skin fibroblasts (D) were cultivated in normal medium (P), under low serum conditions for 6-9 days (Q6, Q7, Q9) followed by serum re-stimulation for 38 hours (Q9→P), or passaged in culture until reaching replicative senescence (S). Cells were processed for immunofluorescence microscopy (confocal images are shown. Bars, 10 μm) or immunoblotting of cell lysates (B, left panel). Samples were analyzed using antibodies against the indicated antigens or stained for senescence-associated β-galactosidase activity (SA β-gal). For testing mRNA levels (B, upper right panel), semiquantitative RT-PCR was performed using primers for indicated cDNAs. Ethidium bromide-stained agarose gels of PCR fragments are shown. In order to test proteasomal degradation of LAP2α (B, lower right panel), cells were starved in low serum medium for 4 days and incubated with or without proteasome inhibitor MG-132 during the last 12 hours. Proteins were precipitated from lysates using LAP2α antibody or hybridoma medium (DMEM) as a control, and immunoprecipitates (P) and supernatants (SN) were analyzed by immunoblotting using antibodies against LAP2α (upper panel) and ubiquitin (lower panel). Input (Inp) represents 1.5% of protein used for IPs. Black and white arrowheads point to ubiquitylated LAP2α. Note, that the ubiquitin blot is weak because of the large background detected in the region >110 kDa. Numbers indicate molecular masses of marker proteins in kDa; mLINT-25, monomeric LINT-25; dLINT-25, dimeric LINT-25; La, lamin; Ubi-LAP2α, ubiquitylated LAP2α; pRb, retinoblastoma protein.

immunofluorescence microscopy revealed a striking upregulation of LINT-25 protein in quiescent cells, concomitant with a strong downregulation of LAP2α and Rb. By contrast, the expression levels and localization of lamin A/C and tubulin remained unchanged. Upon re-stimulation of cell proliferation by addition of serum, original expression levels were fully re-established (Fig. 4A). Thus, protein levels of LINT-25 and LAP2α showed inverse and reversible regulation upon transition to quiescence. To show whether expression changes are caused on the transcriptional or post-transcriptional level, we prepared mRNA from proliferating and quiescent cells and analyzed LAP2α and LINT-25 mRNA

levels by semi-quantitative RT-PCR. Whereas LAP2α mRNA levels remained unchanged, LINT-25 transcripts were upregulated approximately threefold in quiescence (Fig. 4B, top right). Thus LAP2α expression is controlled on the post-transcriptional level, whereas LINT-25 upregulation in quiescence involves transcriptional control. To gain more insights into possible pathways affecting LAP2α protein levels upon cell cycle exit, we analyzed the involvement of proteasome-mediated protein degradation. BJ1 cells were kept in low serum medium for 4 days, during which LAP2α was progressively lost but still detectable, and the proteasome inhibitor MG-132 was added for the last 12 hours in order to transiently inhibit proteasomal degradation and to accumulate ubiquitylated proteasomal target proteins. LAP2α was immunoprecipitated from lysates of MG-132-treated and mock-treated cells and tested by immunoblot analyses using antibodies against LAP2α and ubiquitin (Fig. 4B, lower right). Unlike in the control, the LAP2α antibody recognized a band of around 100 kDa in inhibitor-treated samples in addition to the 75 kDa LAP2α band (Fig. 4B, white arrowhead). A protein migrating at the same position was also faintly labeled with an antibody against ubiquitin (Fig. 4B, black arrowhead), suggesting that it corresponded to an ubiquitylated form of LAP2α. Thus, downregulation of LAP2α in quiescence may involve its ubiquitylation and subsequent proteasomal degradation.

To test whether the inverse regulation of LAP2α and LINT-25 expression can also be seen upon entry of cells into senescence, an irreversible cell cycle exit (Campisi, 2005), we passaged primary human skin fibroblasts in culture until they reached replicative senescence as determined by the upregulation of a senescence-associated β-galactosidase activity (SA-β-gal) (Dimri et al., 1995) (Fig. 4C). Similar to quiescent cells, in senescent cells LINT-25 was clearly upregulated over proliferating controls, and conversely, LAP2α was downregulated to undetectable levels. Again, phosphorylated RbS780 was downregulated, whereas lamin A/C levels remained unchanged. Thus, upregulation of LINT-25 and concomitant downregulation of LAP2α correlated strictly with a non-proliferative state.

In view of the association of LINT-25 with chromatin (see Fig. 3) we wondered how LINT-25 upregulation relates to the chromatin reorganization reported during cell cycle exit in mouse fibroblasts (Grigoryev et al., 2004). Therefore, we analyzed LINT-25 expression and localization in primary mouse skin fibroblasts. Cells were kept in low serum for 6 days to reach quiescence or passaged in culture until they reached replicative senescence, identified by SA β-gal activity (Fig. 4D). Similar to human cells, LINT-25 was dramatically upregulated in quiescent and senescent, Ki67-negative mouse fibroblasts, while LAP2α was downregulated to undetectable levels. Strikingly, however, LINT-25 was reorganized from a uniform, punctate distribution in proliferating cells to clearly defined larger structures in quiescent cells, which were chromocenters of constitutive heterochromatin brightly stained by DAPI (Fig. 4D). Heterochromatin-associated protein HP1α relocalized from the chromocenters to a more diffuse nuclear staining in non-dividing cells as previously described (Grigoryev et al., 2004). All quiescence-related changes in LAP2α and LINT-25 were fully reversible upon readdition of serum to serum-starved cultures (data not shown). Thus, LINT-25 may be involved in chromatin reorganization during cell cycle exit.

Expression levels and localization of LINT-25 also change during differentiation

Having shown that LINT-25 and LAP2α were inversely regulated upon quiescence and senescence-linked cell cycle exit we investigated whether these proteins are regulated similarly during terminal differentiation, which is also linked to irreversible cell cycle exit. Mouse fetal-liver-derived primary erythroid progenitors (EPs) have been shown to undergo highly synchronous in vivo-like erythroid differentiation upon replacement of self renewal factors with physiological differentiation factors, resulting in enucleated erythrocytes (Dolznig et al., 2005). As proliferating EPs expressed both LINT-25 and LAP2α proteins at high levels, we used these cells as an in vitro differentiation model. EPs were switched to erythroid differentiation medium and analyzed by immunoblotting and indirect immunofluorescence microscopy after 24-72 hours (Fig. 5A). Cells stopped proliferating after 24-48 hours, as judged by lack of PCNA and Ki67 staining and accumulation of hypophosphorylated Rb. After 72 hours most cells had expelled their nuclei, but free nuclei were still present in the samples (data not shown). LINT-25 protein was significantly upregulated upon cell cycle exit, reaching a maximum expression level at approximately 48 hours, just before enucleation, whereas LAP2α was continuously downregulated (Fig. 5A). By contrast, LAP2β and lamin A/C levels did not significantly change during differentiation.

Upon differentiation of C2C12 myoblasts into myotubes, we did not observe such a strong upregulation of LINT-25 protein levels, but we detected a profound relocalization from a diffuse pattern to chromocenters upon differentiation (Fig. 5B). LAP2α and Ki67 were downregulated in non cycling myotubes, whereas lamins A/C and HP1α remained unchanged. In conclusion, LINT-25 upregulation and/or relocalization to chromocenters also occurred upon cell cycle exit during differentiation and correlated with LAP2α downregulation.

LINT-25 expression changes during the cell cycle in proliferating cells

Next we wondered whether LINT-25 and LAP2α protein levels may also vary during the cell cycle in proliferating cells. Therefore, we separated BJ1 cells according to their cell cycle phase by centrifugal elutriation. DNA flow cytometry revealed the presence of only G1 phase cells in the early fractions (3.9), whereas the later fractions contained increasing numbers of S-, G2- and M-phase cells (Fig. 6A). Owing to the high proportion of G1 cells in asynchronously growing cells (Fig. 6A, log), all fractions contained contaminating G1-phase cells. Nevertheless, western blot analyses of cell lysates revealed decreasing LINT-25 protein levels from G1 to G2-M phase. By contrast LAP2α protein levels did not change significantly during cell cycle progression.

In addition, we arrested WI-38 human fibroblasts at the G1-S transition by an overnight incubation with the DNA polymerase inhibitor aphidicolin and then allowed the cells to proceed into S phase by removing aphidicolin for 0-24 hours. Again, we detected a decrease of LINT-25 protein level upon

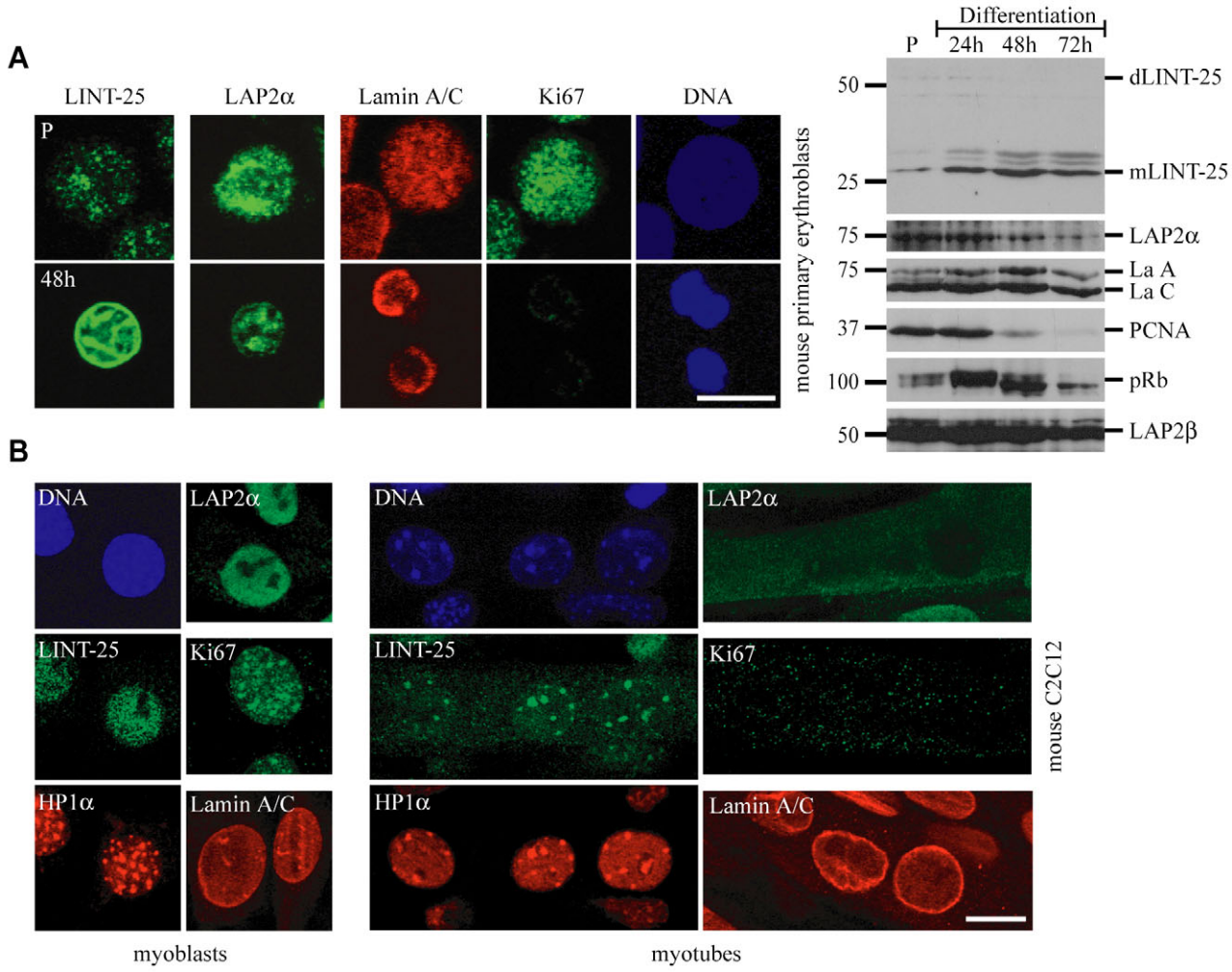

Fig. 5. LINT-25 is upregulated during differentiation. (A) E14.5 fetal liver-derived proliferating erythroid progenitors were switched to erythroid differentiation medium and processed for immunoblotting or immunofluorescence microscopy at the indicated time points, using antibodies as indicated. Numbers indicate molecular masses of marker proteins in kDa; mLINT-25, monomeric LINT-25; dLINT-25, dimeric LINT-25; La, lamin; pRb, retinoblastoma protein. (B) C2C12 myoblasts or myotubes differentiated in 1% FCS for 10 days were processed for immunofluorescence microscopy using antibodies against the indicated antigens. Confocal images are shown. Bars, 10 μm.

exit from the cell cycle block, while LAP2α protein levels remained unchanged (Fig. 6B). Thus, unlike LAP2α, LINT-25 protein levels were increased during G1 phase and declined in S and G2 phase in cycling cells.

LAP2α is not required for LINT-25 dynamics but LINT-25 may regulate LAP2α expression

Our data show a cell cycle exit-dependent inverse change in the expression of LINT-25 and LAP2α, and a redistribution of LINT-25 to chromocenters. To investigate a functional link between these proteins, we analyzed whether changes in the expression of one protein can affect the expression and dynamics of the other protein. In order to test whether LAP2α functions upstream of LINT-25, we analyzed senescence-related changes in LAP2α-deficient primary skin fibroblasts, derived from LAP2α knockout mice (B.K., N.N., C. Stewart and R.F., unpublished data). These cells readily enter senescence after continued passaging as indicated by the SA β-gal staining and by the downregulation of Ki67 (Fig. 7A). Similar to wild-type cells, LINT-25 was found to be upregulated in senescent cells and to accumulate in chromocenters, indicating that LAP2α is not required for cell cycle exit during senescence or for LINT-25 upregulation and relocalization.

Alternatively, LINT-25 may act upstream of LAP2α. To test this possibility, we aimed at changing the expression level of LINT-25 in fibroblasts, but neither stable RNA interference-mediated downregulation of endogenous LINT-25 nor stable expression of ectopic protein was successful, indicating that a well controlled and balanced expression of LINT-25 is essential for cell viability. Intriguingly, however, in a small pool of transfected cells, which did not show signs of apoptosis 15 hours post transfection, we observed a striking downregulation of LAP2α upon LINT-25 overexpression, whereas the expression of GFP alone did not affect LAP2α levels (Fig. 7B). These data could be interpreted in two ways: LINT-25 overexpression may force cells into a non proliferative (=G0) cell cycle stage, which as a secondary effect

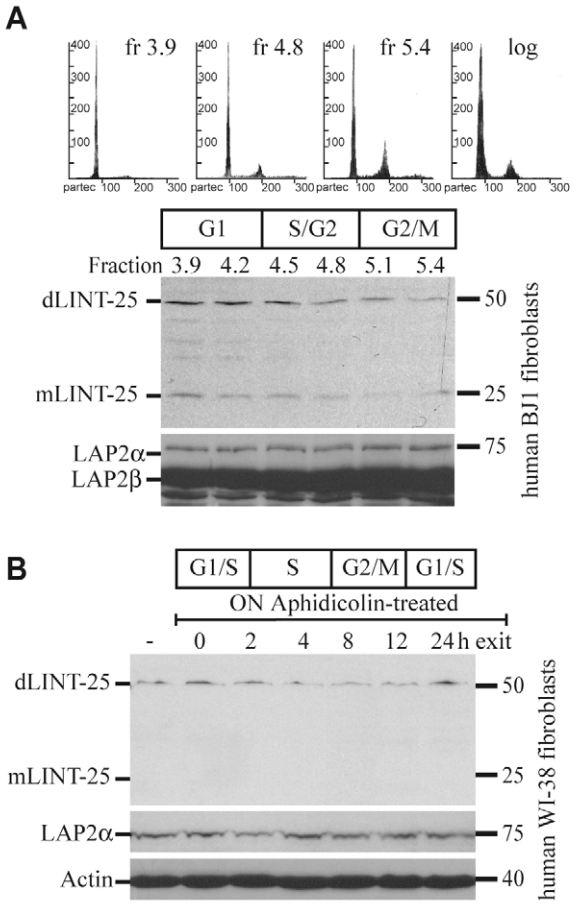

Fig. 6. LINT-25 protein levels change during the cell cycle of proliferating cells. (A) BJ1 cells at different phases of the cell cycle were prepared by centrifugal elutriation and cell fractions were analyzed by DNA flow cytometry. Cell lysates were processed for immunoblotting using antibodies against LINT-25 and LAP2. FACS profiles from representative fractions and from an asynchronous culture (log) are shown. (B) WI-38 human lung fibroblasts were synchronized by an overnight aphidicolin block and released from the block for indicated time periods. Samples were processed for immunoblotting after the indicated time points and analyzed using antibodies against LINT-25, LAP2α and actin. The first lane (–) is a sample from untreated control cells; numbers on the right are molecular masses of marker proteins in kDa; mLINT-25, monomeric LINT-25; dLINT-25, dimeric LINT-25.

causes downregulation of LAP2α. Alternatively, LINT-25 may more directly affect the stability of LAP2α. To distinguish these possibilities we tested whether LINT-25-overexpressing cells were still in a proliferating state, using a Ki67 staining. Similar to the control cells expressing GFP, the majority of LINT-25-overexpressing cells were positive for Ki67 (Fig. 7B), demonstrating that LAP2α downregulation in LINT-25-expressing cells was not due to entry of the cells into a G0 phase, but rather due to a direct effect of LINT-25 on LAP2α.

Altogether, our study identified a novel LAP2α binding partner, which functions upstream of LAP2α, affecting its expression or stability and possibly functioning during entry of cells into a non-proliferative state.

Discussion

In this study we describe a novel nuclear interaction partner of LAP2α, termed LINT-25, which is upregulated during G1 phase of cell proliferation and upon cell cycle exit during quiescence, senescence and differentiation. This is accompanied by translocation of LINT-25 to heterochromatic foci and downregulation of LAP2α. We further show that LINT-25 upregulation is not dependent on LAP2α, but instead LINT-25 acts upstream of LAP2α and may regulate its function in cell cycle-exit pathways.

What is the potential role and relevance of the LAP2α-LINT-25 interaction?

We have recently shown that nucleoplasmic complexes of LAP2α and lamin A/C control cell cycle progression in a Rb-dependent manner. Increased levels of LAP2α delay G1-S phase transition in cycling cells (Vlcek et al., 2002) and re-entry into the cell cycle after serum starvation, whereas LAP2α downregulation interferes with cell cycle arrest upon serum starvation or contact inhibition (Dorner et al., 2006). This cell cycle regulatory activity is mediated by the binding of Rb-LAP2α-containing complexes to E2F promoter sequences, delaying the expression of E2F target genes by yet unknown mechanisms. Despite the cell cycle-inhibiting activity of LAP2α, the protein is highly expressed in proliferating cells, but it is completely absent in non-cycling cells (shown here and in a previous study) (Markiewicz et al., 2002). Thus, rather than being involved in proliferation or maintenance of the non-cycling state, LAP2α may primarily be involved in the transition step from the active cell cycle to a non-cycling state. We propose a model, in which LINT-25 plays a role in regulating LAP2α stability, localization, or function at the G1-G0 transition.

We have previously postulated that the function of nucleoplasmic LAP2α-lamin A/C complexes at the transition from proliferation to the non-cycling state is highly relevant for the molecular mechanisms of laminopathic diseases (Gotzmann and Foisner, 2006). The deregulation of the cell cycle control function of the complex, caused by mutation in lamin A/C or LAP2α, could disturb the sensitive balance between proliferation and differentiation in adult stem cells. This could lead to less efficient tissue regeneration and ultimately to the late onset tissue pathology in patients. Since both LAP2α and LINT-25 are strongly expressed in tissues with high regenerative and proliferative potential, including bone marrow and testis, it is likely that LINT-25 also contributes to tissue regeneration together with LAP2α.

How does LINT-25 affect LAP2α?

Our data indicate that LINT-25 acts upstream of LAP2α. Although we have not been able to demonstrate the existence of a LINT-25-LAP2α complex in living cells because of the insolubility of LAP2α in physiological buffers and the poor performance of the LINT-25 antiserum in immunoprecipitation assays, we consider it very likely that this complex exists at least transiently during cell cycle exit in living cells, for the following reason. Several binding assays and a yeast two-hybrid approach unambiguously demonstrated a direct binding of LINT-25 to LAP2α in vitro and in yeast cells. The data presented here are consistent with a model in which binding of LINT-25 can cause loss of LAP2α by destabilizing the protein,

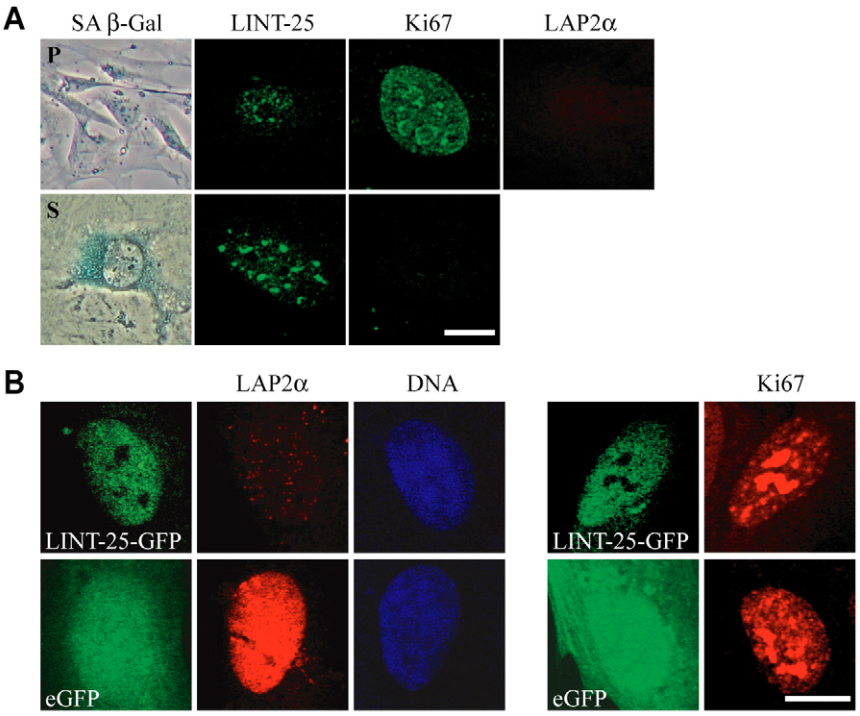

Fig. 7. LINT-25 acts upstream of LAP2α. (A) Primary skin fibroblasts from LAP2α knock-out mice were passaged in culture until senescence (S) and processed for immunofluorescence microscopy together with proliferating control cells (P) using antibodies against LINT-25, LAP2α or Ki67. (B) GFP-tagged LINT-25 (upper panel) or eGFP alone (lower panel) were transiently expressed in BJ1 cells and samples were processed for immunofluorescence microscopy 15 hours after transfection using antibodies against Ki67, LAP2α and Hoechst dye (blue). Confocal images are shown. Bars, 10 μm.

thus contributing to the proper timing of cell cycle exit. As downregulation of LAP2α may be mediated by the ubiquitin-proteasome pathway, it is tempting to speculate that LINT-25 may favor ubiquitylation of LAP2α, although the molecular mechanisms are not known yet. The binding of LINT-25 to, and its effect on, LAP2α may depend on LINT-25 protein level, as LINT-25 was upregulated during cell cycle arrest, and overexpression of LINT-25 led to downregulation of LAP2α. Interestingly, LINT-25 expression levels also changed in cycling cells, being highest during G1 phase. However, LAP2α protein levels were not affected in G1 phase. Therefore, changes in LINT-25 levels within a physiological range may not be sufficient to induce LAP2α downregulation but may require additional signals promoting cell cycle exit. By contrast, massive overexpression of LINT-25 may overcome this requirement. Thus, LINT-25 expression levels may have to be tightly regulated for proper cell cycle timing.

Does LINT-25 have a role in chromatin organization?

Interestingly, the upregulation of LINT-25 upon cell cycle exit was accompanied by its translocation into heterochromatin foci, also called chromocenters. Chromocenters are clusters of centromeres and pericentromeric regions, which form large blocks of constitutive heterochromatin (Grigoryev et al., 2006). Pericentric heterochromatin is composed mainly of long stretches of repetitive DNA sequences and is characterized by the existence of several epigenetic 'marks', including methylation of CpG dinucleotides, hypoacetylation and specific methylation of core histones and enrichment in HP1 (Maison and Almouzni, 2004). Although constitutive heterochromatin is presumed to be stable and independent of the state of cell differentiation or proliferation, recent findings have demonstrated a surprisingly dynamic feature of this type of heterochromatin in vivo during transitions between quiescent and cycling states (Baxter et al., 2004; Grigoryev et al., 2004). Repressive factors, such as HP1 and Ikaros, relocate from chromocenters in proliferating cells to take on a diffuse distribution throughout the nucleus in quiescent cells (Grigoryev et al., 2004). As LINT-25 localizes to pericentric heterochromatin predominantly in non-proliferating cells, one could speculate that it either plays a role in the extensive chromatin reorganizations upon cell cycle exit and/or is involved in the maintenance of the repressive condensed chromatin state of quiescent or differentiated cells. Our observation that LINT-25 relocalizes to chromosomes during early post-mitotic stages of nuclear reassembly supports a role of the protein in chromatin organization. This function of LINT-25, however, is most likely independent of its binding to LAP2α, as these proteins exhibited clearly different chromatin association patterns during nuclear reassembly (Dechat et al., 2004; Vlcek et al., 1999) and, unlike LINT-25, LAP2α was not found in chromocenters at any cell cycle stage. Overall, LINT-25 may have unique, as well as LAP2α-linked, functions in chromatin organization and cell cycle control. This is also reflected by the different expression patterns of these proteins during evolution. Whereas LINT-25 is found in all vertebrates, LAP2α is restricted to mammals (Prufert et al., 2004), Thus, the unique role LINT-25 in chromatin organization may have been conserved in evolution, whereas its role in cell cycle control, in conjunction with LAP2α, may have evolved later.

Materials and Methods

Antibodies

We used the following primary antibodies: monoclonal anti-LAP2 and anti-LAP2α (Dechat et al., 1998); rabbit antisera to LAP2α (Vlcek et al., 2002) and LINT-25 (see supplementary material Fig. S1); and monoclonal antibodies against Myc (1-9E10.2; American Type Culture Collection, CRL-1729); GFP (Roche, Mannheim, Germany); lamins A/C (1E4, a kind gift from Frank McKeon) (Loewinger and McKeon, 1988); lamins A/C (LA-2H10) (Jagatheesan et al., 1999); Rb G3-245 (Pharmingen, San Diego, CA); RbS780 (Cell Signaling Technologies, Beverly); p80coilin (5P10, kindly provided by J. Sleeman, University of Dundee, UK); SC35 (Sigma, Munich, Germany); Ki67 (Novocastra Laboratories Ltd, Newcastle, UK); PCNA (BD Biosciences, San Diego, CA); HP1α (Chemicon, Temecula, CA); α-tubulin (Sigma); and polyclonal anti-lamins A/C antibody N18 (Santa Cruz Biotechnology Inc., Santa Cruz, CA) and anti-ubiquitin (DakoCytomation, Glostrup, Denmark).

LINT-25 antiserum was prepared by immunizing rabbits with urea-solubilized recombinant full-length human LINT-25 with a C-terminal His tag according to standard protocols. For affinity purification, recombinant LINT-25 was blotted and

LINT-25-containing nitrocellulose pieces were incubated with LINT-25 antiserum. Following extensive washing, the antibody was eluted in low pH glycine buffer according to standard protocols.

Yeast two-hybrid screen and construction of expression vectors

The cDNA encoding the LAP2α-specific C-terminus was cloned into pTD16, a modified pAS2-1 plasmid (Clontech Laboratories, Inc., Palo Alto, CA) as described previously (Vlcek et al., 2004) yielding pTD21 that encodes the Gal4 DNA-binding domain fused to LAP2α C-terminus (aa188-693). For the yeast two-hybrid screen, yeast strain PJ69 was cotransformed with pTD21 and a HeLa cDNA library inserted via *Eco*RI and *Xho*I into pGAD-GH (Clontech). Transformants were selected by repeated rounds on SD/–His/–Ade/–Leu/–Trp (SD-HALT) plates. Plasmid DNA was isolated and retransformed into PJ69 together with either pTD21 or pTD16. Plasmids from colonies growing on SD-HALT in the presence of pTD21 but not pTD16 were sequenced from the 5′-end using the Gal4 AD primer. The LINT-25 cDNA-containing plasmid covered the complete coding region except for 6 bp at the 5′ end, and 240 bp of the 3′ non-coding region. The full-length human LINT-25 cDNA fragment was amplified by PCR from the two-hybrid clone using primers 5′-CTAGCTAGCATGGCGGCTCAGCCGCTGCGGCAT-3′ and 5′-CCGCTCGA-GGTTTTCTGGCTTGGACTGGTCAGG-3′ containing the six missing bases, and subcloned into pET-23a(+) (Novagen, Madison, WI), pTD23 (modified pEGFP-N3, for modifications see pTD24) (Vlcek et al., 2002) and pTD6 (modified pUHD10-3) (Vlcek et al., 1999) via the *Nhe*I and *Xho*I sites, to create expression constructs pSH16, pSH13 and pSH17, respectively.

Computer-based analyses

Alignments of homologous LINT-25 cDNA sequences were performed using the BLAST tool (Altschul et al., 1990) of the gene indices databases of the Institute of Genomic Research (www.tigr.org) and the NCBI-Nucleotide database (GenBank; www.ncbi.nlm.nih.gov). Genomic analysis was done using the NCBI-Gene database. Protein primary structure analysis and motif search were performed using ProtParam, InterPro Scan (us.expasy.org) and PredictProtein (Burkhard, 1996).

Reverse transcription-PCR

Human cDNAs made from poly(A)$^+$ RNAs of human tissues or cells were generated and normalized based on actin expression levels as described previously (Brachner et al., 2005). PCR was performed with puRE*Taq* Ready-To-Go beads (Amersham Biosciences, Uppsala, Sweden) using primers specific for human LINT-25 (see above) or LAP2α (5′-GTGGGAACAACCAGGAAGCTATATGA-3′ and 5′-AGA-GTGCTAAGTCCAACTGCTGAT-3′).

Immunoprecipitation and blot overlay assay

Escherichia coli BL21 (DE3) cells were transformed with pSH16 encoding hLINT-25 with a C-terminal His tag. Protein expression was induced with isopropyl-β-D-thiogalactopyranoside (IPTG) for 2-4 hours and recombinant LINT-25 was prepared as described previously (Dechat et al., 1998). Urea-solubilized LINT-25 and LAP2α were dialyzed into binding buffer (50 mM Hepes pH 7.4, 50 mM NaCl, 5 mM $MgCl_2$, 1 mM EGTA, 0.1% Triton X-100, 1 mM DTT, 1 mM PMSF, protease inhibitor mix) and centrifuged at 750 ***g*** for 10 minutes (Heraeus Megafuge 1.0R). Soluble LINT-25 and LAP2α were incubated alone or together at room temperature for 15-30 minutes, mixed with protein G-Sepharose-bound monoclonal antibody against LAP2α (Dechat et al., 1998), and incubated for 30 minutes. Beads were pelleted through 30% sucrose, washed with buffer and analyzed by immunoblotting. Alternatively, LAP2α, LINT-25 and the nucleoplasmic region of LAP2β (1–408) were in vitro translated and labeled with [^{35}S]methionine using plasmids pSH16, pSV5 and pET23a-beta1-408 (Vlcek et al., 1999) in the TNT^R quick coupled transcription/translation kit (Promega, Madison, WI). LINT-25 was incubated alone or together with either LAP2α or LAP2β at room temperature for 30 minutes, diluted 1:8 with binding buffer and precipitated using protein G-Sepharose coupled with monoclonal antibody against LAP2α and LAP2β. For blot overlay assays, recombinant LINT-25 was separated by SDS-PAGE, transferred to nitrocellulose and stained with Ponceau S or India HisProbe-HRP (Pierce, Rockford, IL). For the overlay, the blot was washed in binding buffer, incubated in 1% BSA, and probed with recombinant LAP2α diluted 1:100 in binding buffer overnight at 4°C. After extensive washing, blots were fixed in 0.1% glutaraldehyde for 5 minutes at room temperature, washed in 50 mM NH_4Cl in PBS and processed for immunoblotting.

Subcellular fractionation, gel electrophoresis and immunoblotting

Nuclear and cytoplasmic fractions were prepared as described previously (Dechat et al., 1998). For extraction analyses, 1×10^7 adherent cells were lysed in 400 μl hypotonic buffer with 0.1% Triton X-100, 80 mM iodoacetamide (IAA), and low (10 mM) or high (200 mM) concentration of NaCl for 5 minutes at room temperature. Soluble and insoluble fractions were separated by centrifugation through a 100 μl 30% sucrose cushion for 15 minutes at 750 ***g*** and 4°C (Megafuge 1.0R) and analyzed by immunoblotting. SDS-PAGE and immunoblotting were performed as described previously (Dechat et al., 1998). For testing LINT-25 oxidation, nuclear fractions or whole cells were lysed in Hepes buffer (20 mM Hepes, pH 7.4, 20 mM NaCl, 10 mM $MgCl_2$, 1% Triton X-100, 0.25 mg/ml DNAse I) containing protease inhibitors (1× complete EDTA-free protease inhibitor cocktail, Roche, Mannheim, Germany), different concentrations of DTT (0 mM, 0.1 mM, 10 mM, 100 mM) and the alkylating reagent iodoacetamide (IAA; up to 80 mM), and incubated on ice for 10 minutes.

Cell culture, transfection and centrifugal elutriation

HeLa, hTERT-BJ1 (Clontech Laboratories, Inc., Palo Alto, CA), WI-38 human lung fibroblasts, primary human skin fibroblasts (kindly provided by S. Shackleton, University of Leicester, UK), C2C12 myoblasts and primary mouse skin fibroblasts from wild-type or LAP2α knockout mice (B.K., N.N., C. Stewart and R.F., unpublished data) were maintained at 37°C and 5% CO_2 in Dulbecco's modified Eagle's medium (DMEM) supplemented with 10% fetal calf serum (FCS), 2 mM glutamine, 50 IU/ml penicillin and 50 μg/ml streptomycin (Invitrogen, Carlsbad, CA). For serum starvation, cells were grown in medium with 0.5% FCS for 6-9 days and transferred to medium with 10% FCS for re-stimulation. For proteasome inhibition experiments, 1 μM MG-132 (Calbiochem, La Jolla, CA) was added during the last 12 hours of a 4-day incubation of cells in low serum medium. Cells were lysed in IP buffer (50 mM Hepes pH 7, 4 mM $MgCl_2$, 10 mM EGTA, 100 mM NaCl, 1% Triton X-100, 1 mM DTT, 1 mM PMSF, protease inhibitor mix from Roche, 20 μm cytochalasin B, 0.5 mg/ml DNAse I, 0.2 mg/ml RNAse) and LAP2α was immunoprecipitated using monoclonal antibody against LAP2α or hybridoma medium (DMEM) containing 10% FCS as control (Dechat et al., 2000a). For synchronization, cells were treated with 5 μg/ml aphidicolin (ICN Biomedicals, Ohio) for 18 hours. Staining for β-galactosidase activity was done as described previously (Dimri et al., 1995). Semiconfluent C2C12 myoblasts were differentiated by incubation in medium with 1% FCS for 10 days. Erythroid progenitors from fetal livers of embryonic day (E)14.5 mouse embryos were cultivated and differentiated as described previously (Dolznig et al., 2005). Transient transfections were performed using Lipofectamine 2000 (Invitrogen) according to the manufacturer's instructions. Centrifugal elutriation was performed in a Beckmann JE-6B rotor equipped with a standard separation chamber (Beckmann, Fullerton, CA) at 5°C as described previously (Dolznig et al., 2004). DNA flow cytometry, using a Partec PAS II flow cytometer, was as described by Dorner et al. (Dorner et al., 2006).

Immunofluorescence microscopy

Cells were fixed in 3.7% formaldehyde in PBS for 20 minutes at room temperature, followed by incubation in 50 mM NH_4Cl in PBS and 0.5% Triton X-100 in PBS, for 5 minutes each. After blocking in 0.1% gelatin in PBS for 60 minutes, primary and secondary antibodies conjugated to either Texas Red (Jackson ImmunoResearch, West-Grove, PA) or Alexa Fluor 488 (Molecular Probes, Inc., Eugene, OR) were applied for 1 hour each. DNA was stained with 1 μg/ml Hoechst 33258 for 5 minutes. Samples were mounted in Mowiol and analyzed using a Zeiss Axiovert 200M microscope equipped with a Zeiss LSM510META confocal laser-scanning unit, an αPlan-Fluor 100×1.45 oil (aperture, 0.11 mm) or a Plan-Apochromat 63×1.40 oil DIC MC27 (aperture, 0.19 mm) objective (Zeiss). Images were prepared with Adobe Photoshop software.

We thank Wolfram Goerner, Institute of Biochemistry, University Vienna, for expert technical assistance with the two-hybrid screen, and Thomas Sauer, Max F. Perutz Laboratories, Medical University of Vienna, Vienna, Austria, for assistance with DNA flow cytometry; Sue Shakleton, University of Leicester, UK, for primary human fibroblasts; and Judith Sleeman and Frank McKeon for their gifts of reagents. This study was supported by grants from the Austrian Science Research Fund (FWF, P15312, P17871) to R.F.

References

Altschul, S. F., Gish, W., Miller, W., Myers, E. W. and Lipman, D. J. (1990). Basic local alignment search tool. *J. Mol. Biol.* **215**, 403-410.

Baxter, J., Sauer, S., Peters, A., John, R., Williams, R., Caparros, M. L., Arney, K., Otte, A., Jenuwein, T., Merkenschlager, M. et al. (2004). Histone hypomethylation is an indicator of epigenetic plasticity in quiescent lymphocytes. *EMBO J.* **23**, 4462-4472.

Berger, R., Theodor, L., Shoham, J., Gokkel, E., Brok-Simoni, F., Avraham, K. B., Copeland, N. G., Jenkins, N. A., Rechavi, G. and Simon, A. J. (1996). The characterization and localization of the mouse thymopoietin/lamina-associated polypeptide 2 gene and its alternatively spliced products. *Genome Res.* **6**, 361-370.

Brachner, A., Reipert, S., Foisner, R. and Gotzmann, J. (2005). LEM2 is a novel MAN1-related inner nuclear membrane protein associated with A-type lamins. *J. Cell Sci.* **118**, 5797-5810.

Bridger, J. M., Kill, I. R., O'Farrell, M. and Hutchison, C. J. (1993). Internal lamin structures within G1 nuclei of human dermal fibroblasts. *J. Cell Sci.* **104**, 297-306.

Burke, B. and Stewart, C. L. (2002). Life at the edge: the nuclear envelope and human disease. *Nat. Rev. Mol. Cell Biol.* **3**, 575-585.

Burkhard, R. (1996). PHD: predicting 1D protein structure by profile based neural networks. *Meth. Enzymol.* **266**, 525-539.
Cai, M., Huang, Y., Ghirlando, R., Wilson, K. L., Craigie, R. and Clore, G. M. (2001). Solution structure of the constant region of nuclear envelope protein LAP2 reveals two LEM-domain structures: one binds BAF and the other binds DNA. *EMBO J.* **20**, 4399-4407.
Campisi, J. (2005). Senescent cells, tumor suppression, and organismal aging: good citizens, bad neighbors. *Cell* **120**, 513-522.
Cohen, M., Lee, K. K., Wilson, K. L. and Gruenbaum, Y. (2001). Transcriptional repression, apoptosis, human disease and the functional evolution of the nuclear lamina. *Trends Biochem. Sci.* **26**, 41-47.
Dechat, T., Gotzmann, J., Stockinger, A., Harris, C. A., Talle, M. A., Siekierka, J. J. and Foisner, R. (1998). Detergent-salt resistance of LAP2alpha in interphase nuclei and phosphorylation-dependent association with chromosomes early in nuclear assembly implies functions in nuclear structure dynamics. *EMBO J.* **17**, 4887-4902.
Dechat, T., Korbei, B., Vaughan, O. A., Vlcek, S., Hutchison, C. J. and Foisner, R. (2000a). Lamina-associated polypeptide 2alpha binds intranuclear A-type lamins. *J. Cell Sci.* **113**, 3473-3484.
Dechat, T., Vlcek, S. and Foisner, R. (2000b). Review: lamina-associated polypeptide 2 isoforms and related proteins in cell cycle-dependent nuclear structure dynamics. *J. Struct. Biol.* **129**, 335-345.
Dechat, T., Gajewski, A., Korbei, B., Gerlich, D., Daigle, N., Haraguchi, T., Furukawa, K., Ellenberg, J. and Foisner, R. (2004). LAP2alpha and BAF transiently localize to telomeres and specific regions on chromatin during nuclear assembly. *J. Cell Sci.* **117**, 6117-6128.
Dimri, G. P., Lee, X., Basile, G., Acosta, M., Scott, G., Roskelley, C., Medrano, E. E., Linskens, M., Rubelj, I., Pereira-Smith, O. et al. (1995). A biomarker that identifies senescent human cells in culture and in aging skin in vivo. *Proc. Natl. Acad. Sci. USA* **92**, 9363-9367.
Dolznig, H., Grebien, F., Sauer, T., Beug, H. and Mullner, E. W. (2004). Evidence for a size-sensing mechanism in animal cells. *Nat. Cell Biol.* **6**, 899-905.
Dolznig, H., Kolbus, A., Leberbauer, C., Schmidt, U., Deiner, E. M., Muellner, E. W. and Beug, H. (2005). Expansion and differentiation of immature mouse and human hematopoietic progenitors. *Methods Mol. Med.* **105**, 323-344.
Dorner, D., Vlcek, S., Foeger, N., Gajewski, A., Makolm, C., Gotzmann, J., Hutchison, C. J. and Foisner, R. (2006). Lamina-associated polypeptide 2alpha regulates cell cycle progression and differentiation via the retinoblastoma-E2F pathway. *J. Cell Biol.* **173**, 83-93.
Foisner, R. and Gerace, L. (1993). Integral membrane proteins of the nuclear envelope interact with lamins and chromosomes, and binding is modulated by mitotic phosphorylation. *Cell* **73**, 1267-1279.
Furukawa, K. and Kondo, T. (1998). Identification of the lamina-associated-polypeptide-2-binding domain of B-type lamin. *Eur. J. Biochem.* **251**, 729-733.
Goldman, R. D., Gruenbaum, Y., Moir, R. D., Shumaker, D. K. and Spann, T. P. (2002). Nuclear lamins: building blocks of nuclear architecture. *Genes Dev.* **16**, 533-547.
Gotzmann, J. and Foisner, R. (2006). A-type lamin complexes and regenerative potential: a step towards understanding laminopathic diseases? *Histochem. Cell Biol.* **125**, 33-41.
Grigoryev, S. A., Nikitina, T., Pehrson, J. R., Singh, P. B. and Woodcock, C. L. (2004). Dynamic relocation of epigenetic chromatin markers reveals an active role of constitutive heterochromatin in the transition from proliferation to quiescence. *J. Cell Sci.* **117**, 6153-6162.
Grigoryev, S. A., Bulynko, Y. A. and Popova, E. Y. (2006). The end adjusts the means: heterochromatin remodelling during terminal cell differentiation. *Chromosome Res.* **14**, 53-69.
Gruenbaum, Y., Margalit, A., Goldman, R. D., Shumaker, D. K. and Wilson, K. L. (2005). The nuclear lamina comes of age. *Nat. Rev. Mol. Cell Biol.* **6**, 21-31.
Harris, C. A., Andryuk, P. J., Cline, S., Chan, H. K., Natarajan, A., Siekierka, J. J. and Goldstein, G. (1994). Three distinct human thymopoietins are derived from alternatively spliced mRNAs. *Proc. Natl. Acad. Sci. USA* **91**, 6283-6287.
Hozak, P., Sasseville, A. M., Raymond, Y. and Cook, P. R. (1995). Lamin proteins form an internal nucleoskeleton as well as a peripheral lamina in human cells. *J. Cell Sci.* **108**, 635-644.
Hutchison, C. J. and Worman, H. J. (2004). A-type lamins: guardians of the soma? *Nat. Cell Biol.* **6**, 1062-1067.
Ivorra, C., Kubicek, M., Gonzalez, J. M., Sanz-Gonzalez, S. M., Alvarez-Barrientos, A., O'Connor, J. E., Burke, B. and Andres, V. (2006). A mechanism of AP-1 suppression through interaction of c-Fos with lamin A/C. *Genes Dev.* **20**, 307-320.
Jagatheesan, G., Thanumalayan, S., Muralikrishna, B., Rangaraj, N., Karande, A. A. and Parnaik, V. K. (1999). Colocalization of intranuclear lamin foci with RNA splicing factors. *J. Cell Sci.* **112**, 4651-4661.
Johnson, B. R., Nitta, R. T., Frock, R. L., Mounkes, L., Barbie, D. A., Stewart, C. L., Harlow, E. and Kennedy, B. K. (2004). A-type lamins regulate retinoblastoma protein function by promoting subnuclear localization and preventing proteasomal degradation. *Proc. Natl. Acad. Sci. USA* **101**, 9677-9682.
Lin, F., Blake, D. L., Callebaut, I., Skerjanc, I. S., Holmer, L., McBurney, M. W., Paulin-Levasseur, M. and Worman, H. J. (2000). MAN1, an inner nuclear membrane protein that shares the LEM domain with lamina-associated polypeptide 2 and emerin. *J. Biol. Chem.* **275**, 4840-4847.
Loewinger, L. and McKeon, F. (1988). Mutations in the nuclear lamin proteins resulting in their aberrant assembly in the cytoplasm. *EMBO J.* **7**, 2301-2309.
Maison, C. and Almouzni, G. (2004). HP1 and the dynamics of heterochromatin maintenance. *Nat. Rev. Mol. Cell Biol.* **5**, 296-304.
Markiewicz, E., Dechat, T., Foisner, R., Quinlan, R. A. and Hutchison, C. J. (2002). Lamin A/C binding protein LAP2alpha is required for nuclear anchorage of retinoblastoma protein. *Mol. Biol. Cell* **13**, 4401-4413.
Markiewicz, E., Ledran, M. and Hutchison, C. J. (2005). Remodelling of the nuclear lamina and nucleoskeleton is required for skeletal muscle differentiation in vitro. *J. Cell Sci.* **118**, 409-420.
Matera, A. G. (1999). Nuclear bodies: multifaceted subdomains of the interchromatin space. *Trends Cell Biol.* **9**, 302-309.
Mattout-Drubezki, A. and Gruenbaum, Y. (2003). Dynamic interactions of nuclear lamina proteins with chromatin and transcriptional machinery. *Cell. Mol. Life Sci.* **60**, 2053-2063.
Moir, R. D., Spann, T. P., Herrmann, H. and Goldman, R. D. (2000a). Disruption of nuclear lamin organization blocks the elongation phase of DNA replication. *J. Cell Biol.* **149**, 1179-1192.
Moir, R. D., Yoon, M., Khuon, S. and Goldman, R. D. (2000b). Nuclear lamins A and B1: different pathways of assembly during nuclear envelope formation in living cells. *J. Cell Biol.* **151**, 1155-1168.
Mounkes, L. and Stewart, C. L. (2004). Structural organization and functions of the nucleus in development, aging, and disease. *Curr. Top. Dev. Biol.* **61**, 191-228.
Ozaki, T., Saijo, M., Murakami, K., Enomoto, H., Taya, Y. and Sakiyama, S. (1994). Complex formation between lamin A and the retinoblastoma gene product: identification of the domain on lamin A required for its interaction. *Oncogene* **9**, 2649-2653.
Prufert, K., Winkler, C., Paulin-Levasseur, M. and Krohne, G. (2004). The lamina-associated polypeptide 2 (LAP2) genes of zebrafish and chicken: no LAP2alpha isoform is synthesised by non-mammalian vertebrates. *Eur. J. Cell Biol.* **83**, 403-411.
Segura-Totten, M., Kowalski, A. K., Craigie, R. and Wilson, K. L. (2002). Barrier-to-autointegration factor: major roles in chromatin decondensation and nuclear assembly. *J. Cell Biol.* **158**, 475-485.
Spann, T. P., Goldman, A. E., Wang, C., Huang, S. and Goldman, R. D. (2002). Alteration of nuclear lamin organization inhibits RNA polymerase II-dependent transcription. *J. Cell Biol.* **156**, 603-608.
Stuurman, N., Heins, S. and Aebi, U. (1998). Nuclear lamins: their structure, assembly, and interactions. *J. Struct. Biol.* **122**, 42-66.
Taylor, M. R., Slavov, D., Gajewski, A., Vlcek, S., Ku, L., Fain, P. R., Carniel, E., Di Lenarda, A., Sinagra, G., Boucek, M. M. et al. (2005). Thymopoietin (lamina-associated polypeptide 2) gene mutation associated with dilated cardiomyopathy. *Hum. Mutat.* **26**, 566-574.
Van Berlo, J. H., Voncken, J. W., Kubben, N., Broers, J. L., Duisters, R., van Leeuwen, R. E., Crijns, H. J., Ramaekers, F. C., Hutchison, C. J. and Pinto, Y. M. (2005). A-type lamins are essential for TGF-beta1 induced PP2A to dephosphorylate transcription factors. *Hum. Mol. Genet.* **14**, 2839-2849.
Vlcek, S., Just, H., Dechat, T. and Foisner, R. (1999). Functional diversity of LAP2alpha and LAP2beta in postmitotic chromosome association is caused by an alpha-specific nuclear targeting domain. *EMBO J.* **18**, 6370-6384.
Vlcek, S., Korbei, B. and Foisner, R. (2002). Distinct functions of the unique C terminus of LAP2alpha in cell proliferation and nuclear assembly. *J. Biol. Chem.* **277**, 18898-18907.
Vlcek, S., Foisner, R. and Wilson, K. L. (2004). Lco1 is a novel widely expressed lamin-binding protein in the nuclear interior. *Exp. Cell Res.* **298**, 499-511.
Williams, J. M., Chen, G. C., Zhu, L. and Rest, R. F. (1998). Using the yeast two-hybrid system to identify human epithelial cell proteins that bind gonococcal Opa proteins: intracellular gonococci bind pyruvate kinase via their Opa proteins and require host pyruvate for growth. *Mol. Microbiol.* **27**, 171-186.